JOURNAL OF APPLIED ELECTROCHEMISTRY 15 (1985) 755–766

An a.c. impedance study of steel in concrete

P. LAY, P. F. LAWRENCE, N. J. M. WILKINS, D. E. WILLIAMS

Materials Development Division, AERE Harwell, Oxfordshire OX11 ORA, UK

Received 19 March 1984, revised 22 October 1985

Impedance measurements executed between both steel and platinum electrodes embedded in both porous and non-porous concretes were used to explore the physical characteristics of the system. A simple method is described for measuring high impedances (up to 500 MΩ) in which the unknown impedance is compared with the input impedance of the measuring instrument, previously calibrated. Impedance measurements on concrete immersed in an electrolyte were used to quantify concrete quality, and the dynamics of wetting, drying and electrolyte exchange were explored: the dynamics of such processes are considered to be amongst the factors determining the rate of corrosion of steel reinforcement under some conditions since intermittent wetting is an efficient method for transporting oxygen and salt into the concrete. The existence of cracks along the electrode–concrete interface was inferred. Impedance changes consequent on the initiation of corrosion of steel electrodes were noted, but the changes were small and not clear-cut.

1. Introduction

In common with many other physical and chemical systems, that of steel in concrete can be represented by an electrical equivalent circuit (Fig. 1) [1]. Identification of the elements in this circuit representing the steel–concrete interface facilitates the study of corrosion processes [2] whilst other elements in the circuit give information concerning the nature of the concrete, particularly its open porosity and, as we show here in a preliminary fashion, the existence of cracks within the concrete and at the concrete–steel interface.

Page and Treadaway [3] have reviewed the current knowledge concerning the behaviour of steel in concrete and the ground is covered in detail in a recent book [4]. In order to illustrate the discussion which follows, a representation of the concrete–steel system [2] is sketched in Fig. 2. Concrete has both open porosity and cracks which allow easy penetration of liquid from the external medium, and closed zones with only a slow penetration of liquid. Water and salts may permeate slowly into the cement phases and slow changes in local solution compositions may result. Penetration of reagents from the environment (CO_2, O_2, Cl^- for example) and diffusion of corrosion products away from the steel may be mainly by means of microcracks. In the vicinity of the steel the very alkaline solution established by the cement (pH ~ 13) is assumed to maintain the stability of the steel against corrosion. Penetration of carbon dioxide tends to cause a decrease in pH and if this occurs to a sufficient degree then corrosion may initiate [5]. Defects in the concrete, developed, for example, during casting, may penetrate to the steel: the reinforcement will be less well protected in these areas and local corrosion attack may be initiated by galvanic action between the poorly protected regions of the steel and the well protected surroundings. At the anodic areas the pH decreases as a result of hydrolysis of iron chloride corrosion products, so the adjacent concrete becomes neutralized and the anodic area extends. The iron hydroxide corrosion products themselves occupy a greater volume than the steel from which they form; the resulting increase in volume can provoke cracking and disintegration of the concrete. In general, however, corrosion rates of reinforcing bars in wet concrete are extremely low and limited by the rate of supply of oxygen from the atmosphere to the steel. Highest corrosion rates are found in circumstances involving intermittent wetting of the concrete since in these circumstances the resistivity of the concrete may be low because of partial saturation with water, whilst the oxygen

0021–891X/85 $03.00 + .12

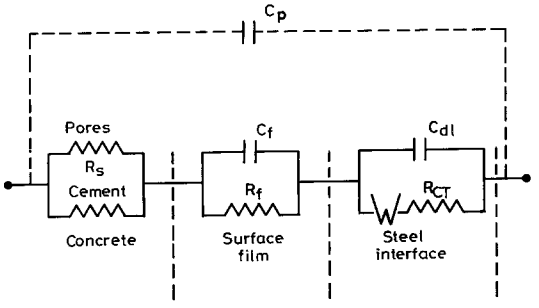

Fig. 1. Conventional equivalent circuit for the steel–concrete system: W, impedance contributed through diffusion of reactants (O_2, Cl^-) to the interface; R_{CT}, impedance contributed by the interface reaction, dissolution of the steel; C_{dl}, capacitance of the electrical double layer at the steel–concrete interface; C_p, capacitance contributed by the specimen geometry and measuring instrument input circuitry. The surface film is assumed to be a layer of rust. The corrosion reaction is assumed to continue under this layer and reactants to diffuse through it.

supply may be high since the solution in the concrete is intermittently replenished by fresh, oxygen-saturated solution. Cracking of the concrete through to the reinforcement is obviously a matter for some concern. Localized corrosion of the steel at a crack, for example, can lead to severe loss of strength without any obvious signs of damage being apparent on the external surface of the structure. Bazant [6, 7] has considered how to set up a mathematical description of the corrosion process.

This paper describes a preliminary attempt to explore some of these aspects of corrosion of reinforcing bars using the a.c. impedance method. Two different grades of concrete incorporating different sizes of aggregate have been studied. Specimens having both steel and platinum electrodes embedded were immersed in sea water and demineralized water and exposed to dry atmospheres and atmospheres of different relative humidity for a period of 2 years before measurements commenced. With other specimens, impedance changes during curing under water and impedance changes upon drying, rewetting and transfer between salt and demineralized water were examined. A novel, simple method of measuring very high impedances was demonstrated.

The results of this work complement those of an earlier study [2] of the behaviour of steel electrodes in poor quality concrete studied over a long period of time. We did not observe a component of the impedance attributable to the development of a surface film on the steel [2], since, in this work, extensive rusting of the steel electrodes did not occur. For the specimens studied here, it was concluded that the impedance behaviour was dominated by cracks in the concrete and at the interface between the electrodes and the concrete. There was, however, one case in which an indication of the initiation of corrosion of steel electrodes was obtained, though not particularly clear cut. The conclusions were confirmed by visual examination of the electrodes after the specimens had been broken open.

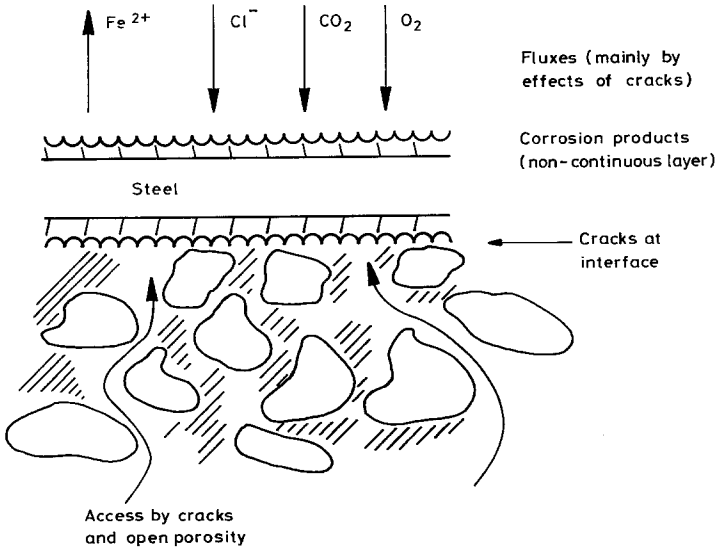

Fig. 2. Simple physical representation of the concrete–steel system.

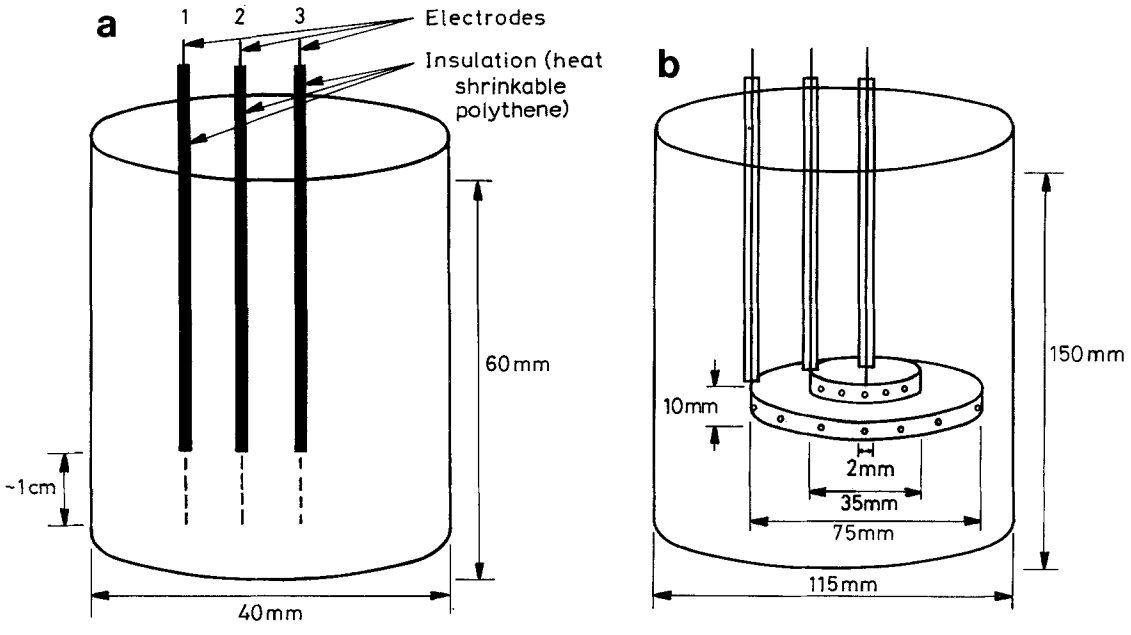

Fig. 3. Concrete specimens: (a) non-porous; (b) porous.

2. Experimental details

2.1. *Concrete specimens*

Two grades of concrete were investigated. One was very carefully prepared with fine aggregate to be free of voids. The other was prepared with coarser aggregate (sieved < 9 mm) and was not well compacted. The non-porous concrete [8] was obtained by mixing graded dry sand and aggregate as follows: 1.2 mm to 2.4 mm, 40 parts; 0.6 mm to 1.2 mm, 15 parts; 0.3 to 0.6 mm, 10 parts; 0.2 to 0.3 mm, 20 parts; less than 0.2 mm, 15 parts by weight. The aggregate was dry mixed in the ratio 3 : 1 by weight with ordinary Portland cement and the resulting mixture compacted with vibration into a mould. The filled mould was saturated with distilled water under vacuum and cured for 1 day at 20° C in water-saturated air. The specimens were then removed from the moulds and further cured for 28 days immersed in distilled water at 20° C. The water : cement ratio, determined by weighing, was 0.55. The porous concrete comprised 5 parts by weight of ballast (< 9 mm), 1 part ordinary Portland cement and 0.5 part water (water: cement = 0.5); it was cast into moulds and allowed to react for 3 days in water-saturated air before being immersed in distilled water to complete curing.

Twelve specimens of the non-porous concrete (Fig. 3a) containing wire electrodes of platinum or steel had been exposed for 2 years either totally immersed in seawater or demineralized water or under a controlled humidity atmosphere. Atmospheres were established by silica gel ($P_{H_2O} \leqslant 0.1$ Torr) and by saturated solutions of $Ca(NO_3)_2$ (relative humidity 51%) or Na_2SO_4 (relative humidity 90%). Six specimens of the porous concrete (Fig. 3b) containing concentric cylindrical steel electrodes were prepared and the evolution of electrical impedance with time as the specimens cured under demineralized water was followed. Two of these specimens were removed from the water after 18 days curing; one of these was allowed to dry out in the laboratory atmosphere whilst the other was immersed in sea water. The dried specimen was also immersed in sea water after a further 10 days. The remaining specimens were cured for 28 days; two of these were allowed to dry and two were immersed in sea water. Impedance variations with time were monitored for all the specimens. Measured resistances were converted

to resistivities using the formula

$$\varrho = R\left[\frac{\pi l}{\ln (a/a_0)}\right] \quad (1)$$

for the specimens with parallel wire electrodes, where ϱ denotes resistivity and R the resistance measured between two parallel wires of length l, radius a_0 and separation a, with $a \gg a_0$, and

$$\varrho = R\left[\frac{2\pi l}{\ln (a_2/a_1)}\right] \quad (2)$$

for the specimens with concentric cylinder electrodes, where R is the resistance measured between two concentric cylinders of length l and radii a_2 and a_1 respectively.

2.2. *Impedance measurements*

Impedance measurements were made using a digital frequency response analyser (FRA) controlled by a microcomputer. The instrument (Solartron type 1174) could measure over the range 10^{-4} to 10^{6} Hz and had an input impedance of 1 MΩ in parallel with 50 pF.

Measurement of high values of impedance tends to be difficult because one is limited by the input impedance of the measuring instrument, and because buffer amplifiers of sufficiently high input impedance may not have the necessary response bandwidth. The problem was solved for this work by, in effect, calibrating the input impedance of the measuring instrument and comparing the unknown impedance with it. The circuit is shown in Fig. 4. If V_y and V_x represent the voltages compared by the FRA then the measured quantities are the real and imaginary parts of the ratio

$$V_y/V_x = A + jB \quad (3)$$

If the unknown impedance is represented as $Z = Z' + jZ''$ and R_i and C_i are the equivalent parallel input resistance and capacitance of the measuring instrument as represented in Fig. 4, then

$$Z' = \frac{R_{in}}{1 + \omega^2 R_{in}^2 C_i^2}(A - 1 + B\omega C_i R_{in}) \quad (4)$$

and

$$Z'' = \frac{R_{in}}{1 + \omega^2 R_{in}^2 C_i^2}[(A - 1)\omega C_i R_{in} - B] \quad (5)$$

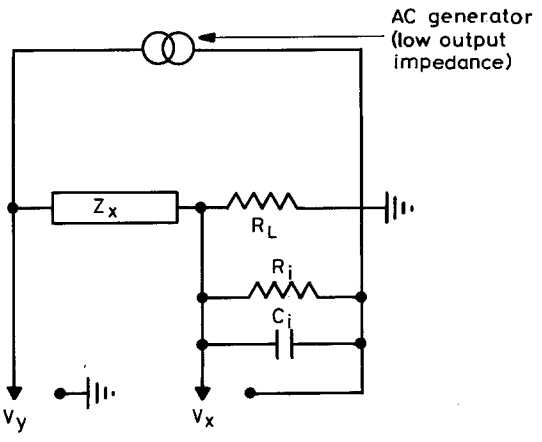

Fig. 4. Measurement circuit. Z_x, unknown impedance; R_L, load resistor (typically 10^7 Ω); R_i and C_i, input impedance of the FRA; V_y and V_x, voltages measured and compared by the FRA.

where $\omega = 2\pi f$ (f being the measurement frequency) and R_{in} is the parallel combination of R_i and R_L. The values of R_i and C_i were computed from the results of measurements in which the unknown impedance, Z, was replaced by standard resistors. Impedances of up to about 500 MΩ could be determined.

The data in this paper are presented using partial Bode diagrams (Fig. 5). In this method the magnitude of the impedance, ($|Z|^2 = Z'^2 + Z''^2$, where Z' denotes the resistive part and Z'' the reactive part of the impedance) is plotted against frequency, f. Different equivalent circuits can be recognized in different shapes of the diagram; changes in resistance move the diagrams parallel to the $|Z|$ axis whereas changes in reactance (capacitance or inductance) cause movement parallel to the frequency axis. The representation is thus very useful for bringing out, for example, changes in circuit elements with time.

3. Results

3.1. *Non-porous concrete*

Fig. 6 shows some results of impedance measurements on the 'non-porous' concrete. These diagrams show a high frequency relaxation due to the geometrical capacitance of the specimen (1–2 pF, C_p in Fig. 1) and a low frequency relaxation due to the capacitance associ-

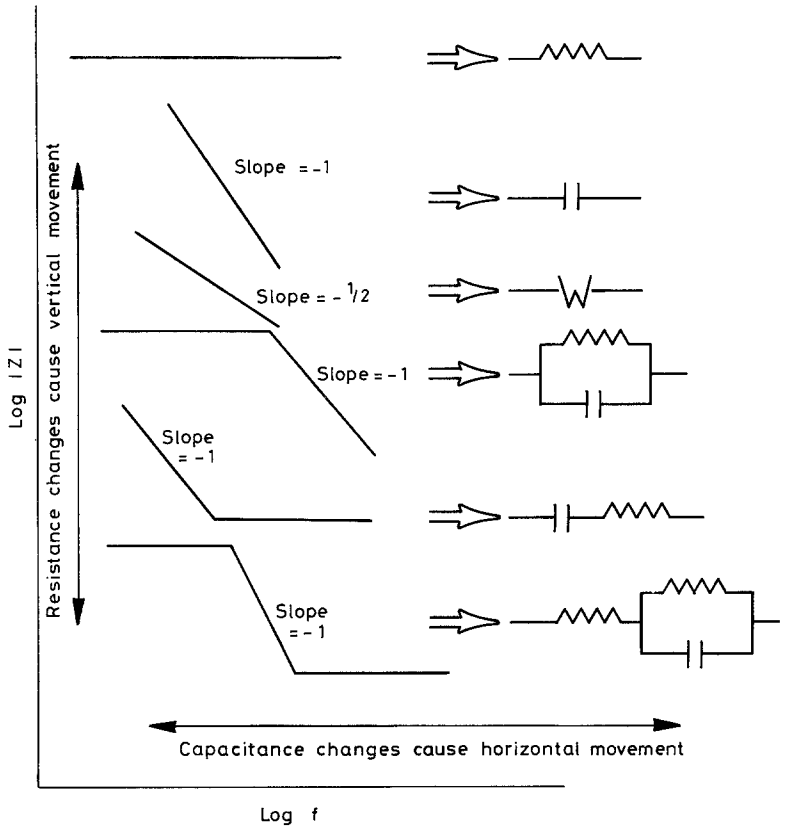

Fig. 5. Impedance analysis with Bode diagrams.

ated with the concrete–steel interface (C_{dl} in Fig. 1), the two relaxations being separated by a section of constant impedance due to the resistance of the concrete between the electrodes (R_s in Fig. 1). The interface capacitance for the immersed specimens was around 20–50 μF cm^{-2} whilst for the non-immersed specimens it was probably about 0.1 μF cm^{-2}. For some of the immersed specimens at very low frequency the diagram again tended to a constant impedance attributable to the charge-transfer resistance across the interface (R_{CT} in Fig. 1). The representation of the interface capacitance as a simple capacitor is clearly an approximation; the slope of the low frequency relaxation was typically -0.7 to -0.8, not -1 as expected for a simple capacitor and as observed for the high frequency relaxation.

In each class of specimen the concrete resistance varied greatly from one specimen to another. A simple explanation for this is that there was a small number of small cracks in the specimens. The resistance of specimens immersed in sea water was in general lower than the resistance of those immersed in distilled water.

3.2. *Porous concrete*

3.2.1. Impedance evolution during curing. Fig. 7 is a Bode representation showing the evolution of the impedance with curing time. During the curing period there was little change in impedance of any of the specimens although there were variations in the magnitude of the impedance from one specimen to another, particularly with measurements made to the central rod. The resistivity of the concrete increased slightly during the curing process.

3.2.2. Impedance variation with drying time. The time evolution of the Bode diagram of a specimen following its removal from demineralized water after 18 days of curing is shown in Fig. 8. Both resistivity and capacitance changes were observed. The results depended upon which elec-

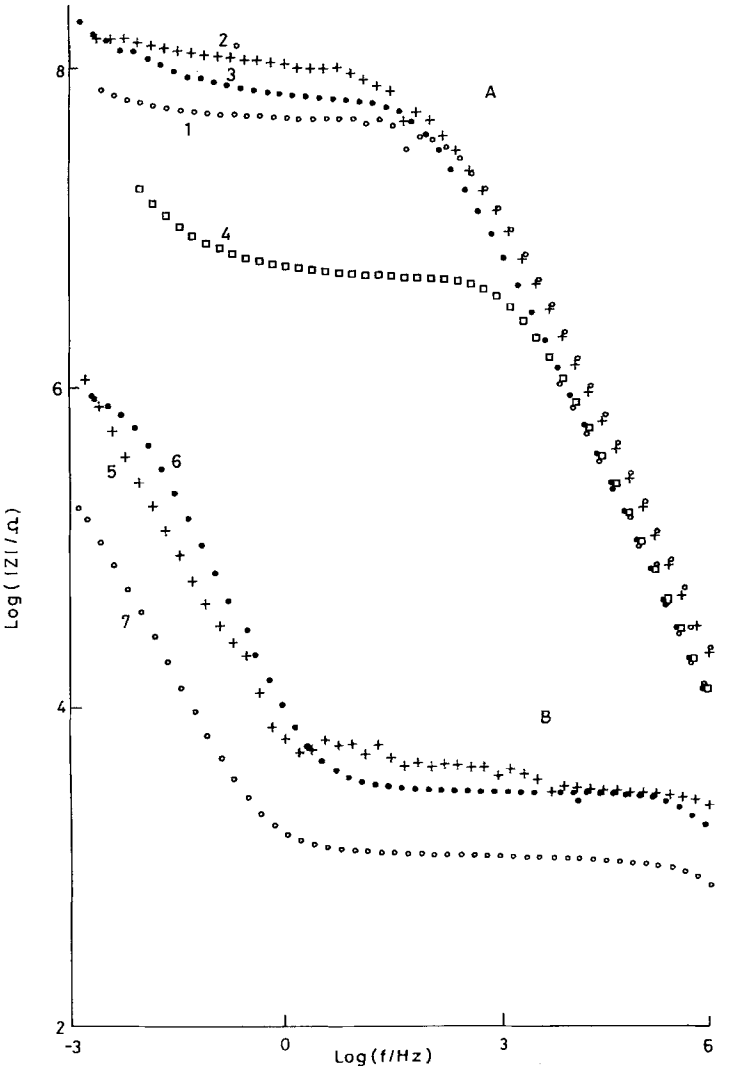

Fig. 6. Representative impedance diagrams for non-porous concrete. Impedance modulus, $|Z|$, against signal frequency, f. A – unimmersed specimens; B – immersed specimens: 1, dry; 2, 90% RH; 3 and 4, 50% RH (two different specimens); 5, demineralized water, two steel electrodes; 6, demineralized water, one steel and one platinum electrode; 7, seawater, two steel electrodes.

trode pair was chosen and were different for different specimens. One specimen in particular showed a very sudden, large increase in resistivity after 5 days.

3.2.3. Replacement of demineralized water with sea water. The resistance fell and the apparent interface capacitance increased with time. Both reached a stable value within 1 day (Fig. 9).

3.2.4. Re-immersion of a dry specimen in sea water. When a dried specimen was re-immersed in sea water the resistivity fell to a stable value within 30 min (Fig. 9). A change in the interface impedance manifested by a reduction in the slope of the low frequency relaxation occurred over a period of about 12 days after re-immersion (Fig. 10). When this specimen was broken open the electrodes were observed to have started corroding.

4. Discussion

4.1. *Non-porous concrete*

4.1.1. Unimmersed specimens. The unimmersed specimens can be represented as a high value resistor, i.e. the resistance of the concrete, in parallel with a small capacitance relating to the geometry of the system. At very low measurement frequencies there was the first sign of a relaxation which could relate to the metal–con-

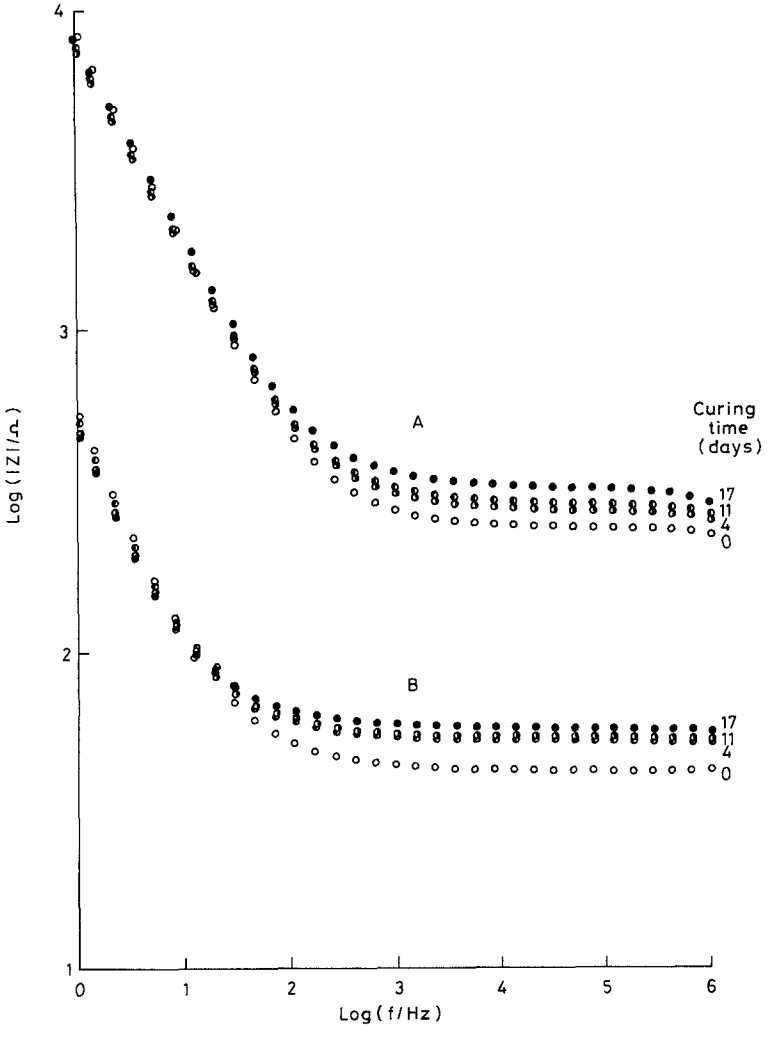

Fig. 7. Evolution of impedance during curing of porous concrete. A, inner ring to central rod; B, outer ring to inner ring; parameter, curing time (days).

crete interface. There was no obvious systematic variation with the humidity of the atmosphere. The variability from one specimen to another and the observation that some specimens had a resistance > 500 MΩ implies that the impedance was dominated by small cracks at the metal–concrete interface. In other words the concrete did not make a good contact with the metal. Microscopic cracks, both at the interface and within the bulk of the concrete would give rise to a capacitive component of the impedance.

4.1.2. Immersed specimens. The capacitance values observed for the immersed specimens (geometrical area of electrodes $\sim 1\,cm^2$) are similar to values of double layer capacitance observed at metal electrodes in electrolyte solutions. One might expect that if the amount of free electrolyte at the metal–concrete interface were small, rather smaller values of capacitance would be observed. If the capacitance were due to some surface layer of corrosion product smaller values again might be expected. One simple explanation is that there was a substantial amount of free electrolyte at the metal–concrete interface; in other words the interface was extensively cracked, as postulated for the dry concretes above. The interfacial capacitance cannot be represented as a simple ideal capacitor: the slope of the Bode diagram would in that case be just -1 as it is for the high frequency relaxation of the dry concrete. If the interface were in fact a system of cracks filled with electrolyte then it could be represented as a distri-

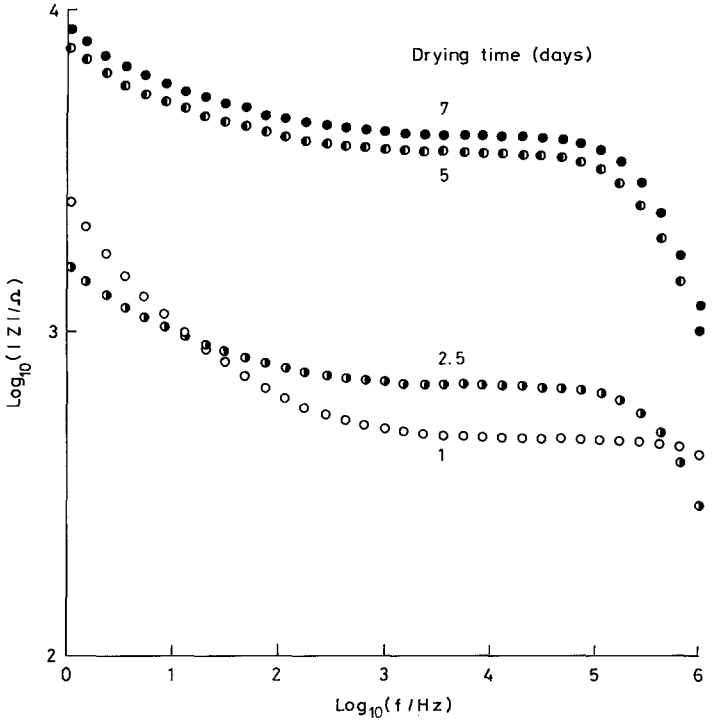

Fig. 8. Evolution of impedance on drying of porous concrete: measurements between inner ring and central rod. Parameter, time in days after removal from demineralized water.

buted network. Such circuits have slope less than one in the Bode diagram. With such a distributed network the larger apparent value of the interface capacitance for specimens immersed in sea water could be related simply to the lower resistance of the electrolyte in the pores and cracks. Extensive cracking at the metal–concrete interface is perhaps to be expected, especially with a smooth metal surface as here. When a specimen was broken open at the end of the test there was no adhesion of the concrete to the metal surface at all. The metal was bright and shiny; no trace of corrosion was evident.

4.1.3. Corrosion of steel electrodes. The corrosion rate of the steel may be estimated from the value of the polarization resistance of the interface, R_p

$$i_c = b/R_p \qquad (6)$$

where b denotes the Tafel parameter and i_c the corrosion current. R_p here is the zero frequency, or d.c. value of the impedance. In the notation of Fig. 1 it is the sum of R_{CT} and W. It is assumed that the corrosion rate is limited by diffusion of oxygen to the interface, so b could be quite large and in theory would approach infinity (current independent of applied potential). The polarization resistance of the steel in these specimens was at least $10^6\,\Omega\,cm^{-2}$, so arbitrarily taking $b = 0.2\,V$ as a typical large value for reaction approaching diffusion control, the corrosion current was probably less than $2 \times 10^{-7}\,A\,cm^{-2}$, equivalent to a corrosion rate of less than $2\,\mu m$ per year.

Comparison of the response of platinum and steel electrodes did not show any feature which might have been interpreted in terms of corrosion of the steel. In fact when one specimen which had been immersed in sea water for 2 years was broken open the surfaces of the steel electrodes were as bright and shiny as they were when the specimens were originally prepared.

4.2. *Porous concrete*

4.2.1. Impedance evolution during curing. The points to note here are the rather small variation of resistivity with time during the curing process, the lack of specimen-to-specimen variation for measurements made between the two outer rings and the interspecimen variability of results of measurements to the central rod.

The two outer ring electrodes allow a uniform

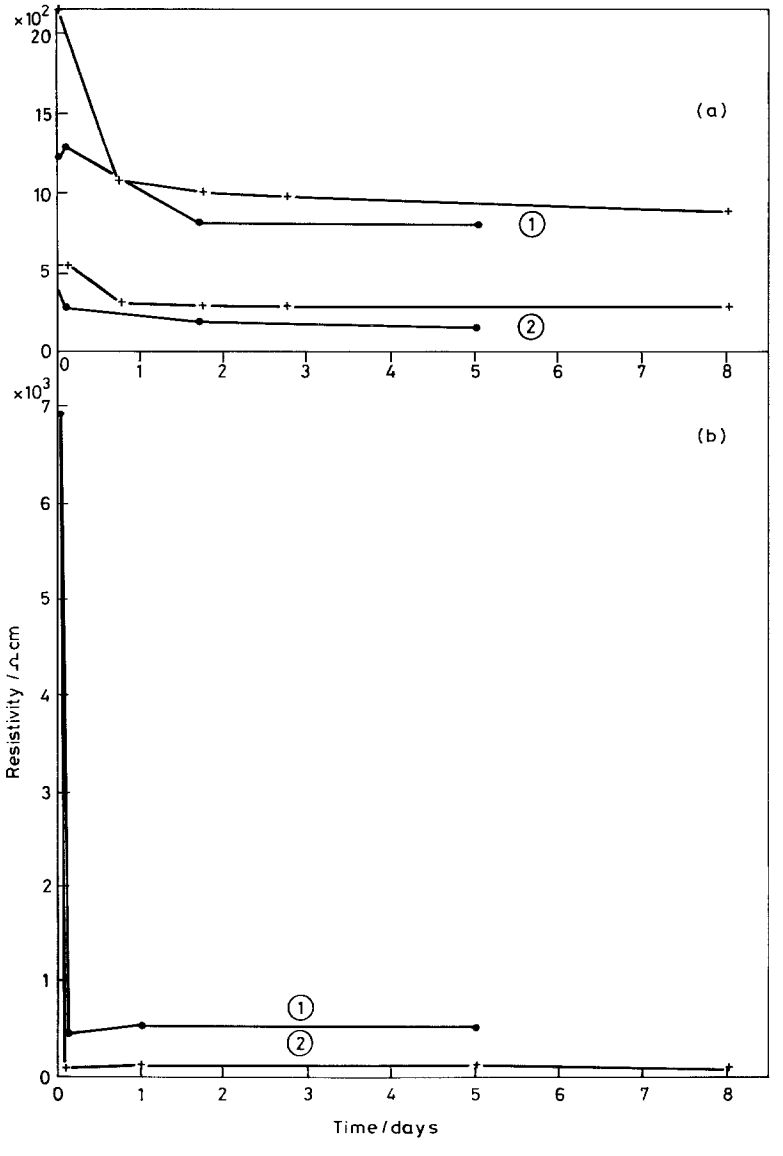

Fig. 9. Resistivity changes after change of bathing fluid for porous concrete: a, demineralized water to seawater; b, dry to seawater. 1, inner ring to central rod; 2, outer ring to inner ring.

and symmetrical flow of current between them. The resistance measured would reflect the value of the lowest resistance paths between the two rings and it is interesting to note that the value is similar for all the samples.Although the geometry is equally symmetrical about the central rod the flow of current is more concentrated there. The measured value of the impedance therefore becomes sensitive to the particular conditions near the rod and could be changed by relatively small effects such as the presence of pieces of ballast, small cracks or porosity. This idea can explain the specimen-to-specimen variability.

The small domain of the evolution of impedance with curing time can be explained by the large porosity of the concrete. For concrete impregnated with electrolyte the conductivity is dominated by the largest open spaces filled with electrolyte and the dimensions of the channels interlinking them (see Section 4.3.). It may be assumed that the curing process resulted in the finer porosity becoming filled with reaction products but that large cracks and voids were unaffected. Since these would dominate the conductivity, the resistivity would not be expected to change much during curing if large enough defects were present. Conversely, a strong varia-

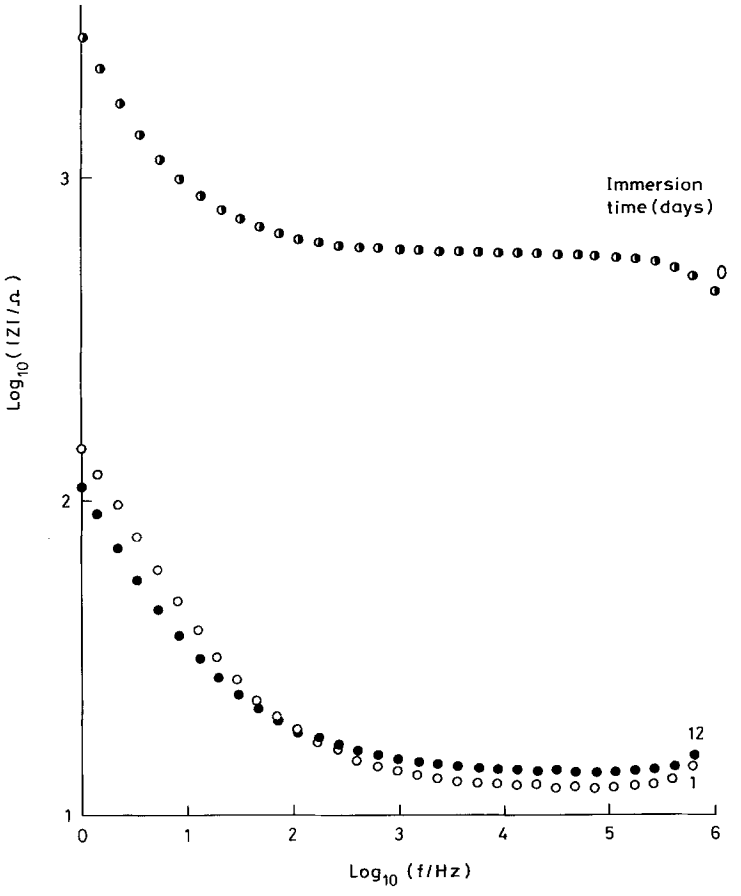

Fig. 10. Evolution of impedance of a dried specimen of porous concrete after immersion in seawater.

tion of conductivity with curing time could be taken to imply the absence of gross defects.

4.2.2. Impedance evolution during drying following curing. The difference between dry and wet concrete can be taken into account by representing the bulk material as two resistors in parallel, one resistor representing the cement phase, the other the electrolyte-filled porosity. These results can be rationalized with the assumption that conduction takes place largely through electrolyte remaining trapped within the porosity. Only when the amount of electrolyte remaining was greatly reduced by evaporation would the conduction proceed via the cement phase. This hypothesis explains why there was an induction time before significant resistance increase occurred. The very sudden increase in resistivity shown by one specimen can be explained by the assumption that the concrete cracked at the interface with the central rod at that time, thus losing contact. This rod in fact did become loose. There was also a time evolution during drying of the interfacial component of the impedance, revealed at low frequencies. This is easily explained if the interfacial impedance is also dominated by cracks, as has been discussed above.

4.2.3. Impedance evolution upon immersion in sea water following curing. The observed resistivity decrease can be interpreted in terms of an increase in the conductivity of the electrolyte filling the large pores of the concrete. Thus the data (Fig. 9) imply that the exchange of the electrolyte took about 1 day. This exchange seems surprisingly fast; if diffusion alone were operating the expected time scale would be about $r^2/2D$, where r denotes the specimen radius and D the salt diffusivity in the concrete. Taking $r \sim 5$ cm and D, computed from the equilibrium conductivity as in Section 4.3., as

about 4×10^{-7} cm^2 s^{-1}, gives $t \sim 10^7$ s (about 100 days).

The rapid variation observed could reflect diffusion along a few rather large cracks. In this case there should be a longer term variation as the rest of the concrete saturated both by way of the cracks as well as by way of diffusion from the outer surface. Other possibilities are that migration of Cl^- inward is driven by a junction potential set up as a result of the diffusion of OH^- outward, or that water flows into the concrete as a result of an osmotic pressure gradient, carrying salt with it.

Observations on concrete structures and large specimens immersed in seawater [4] have shown that penetration of chloride is very slow, i.e. 30–60 mm in 6 months, with very little further penetration. This initial penetration is equivalent to an apparent diffusion coefficient of about 3×10^{-7} cm^2 s^{-1}, a value which is in agreement with the present measurements. It is known that the seawater reacts slowly with cement to precipitate calcium carbonate and magnesium hydroxide or basic magnesium carbonates and it is considered that these precipitates clog up the porosity of the medium and hence reduce the diffusibility. It is clear that resistivity measurements would be a simple and effective method of exploring this phenomenon.

4.2.4. Electrode corrosion upon immersion in sea water following drying. Again these data showed that the electrolyte penetrated the pores of the concrete extremely fast, i.e. within 30 min. Capillary action could have been the force driving this. The magnitude of impedance that resulted was lower than that observed from the specimens which had not been dried. Possibly there had been some further cracking as a result of drying. As has been remarked, the small increase in resistivity and a change in interfacial impedance observed after this specimen had been in seawater some days corresponded to the onset of corrosion of the electrodes. The corrosion reaction would have been accelerated initially because the electrolyte sucked into the dry concrete was oxygen-saturated. It is possible that cracks, formed along the concrete–steel interface as a result of shrinkage during drying, limited the buffer action of the concrete so that the local pH dropped as a result of the corrosion. The corrosion rate should then be further accelerated, although it would remain limited by the rate of oxygen transport for the cathodic process.

The experiment perhaps illustrates phenomena which could occur in zones of concrete marine structures wetted intermittantly, for example, as a result of tidal variations or in the splash zone where, indeed, the highest corrosion rates of steel reinforcement are observed.

4.3. *Porosity of the concrete*

Diffusion of ions through the electrolyte in an electrolyte-saturated porous medium such as concrete can be characterized by three parameters [9] namely: porosity, ε, defined as the volume fraction of electrolyte; constrictivity, δ, expressing the cross-sectional area of the paths connecting the pores; and tortuosity, τ, expressing the total path length through the interconnections through the specimen. If the electrical resistance of concrete immersed in an electrolyte is assumed to be determined by the resistivity of the free electrolyte (ϱ_{free}), concentration, c, modified by the porosity of the concrete, then the apparent diffusion coefficient (D_{app}) of salt through the concrete can be approximately calculated from the measured electrical resistivity,

$$D_{\text{app}} \sim (RT/F^2)(1/c\varrho) \tag{7}$$

Furthermore, a composite parameter, the diffusibility, Q, expressing the resistance of the concrete to diffusion of salts, can be defined

$$Q = \frac{\varepsilon\delta}{\tau^2} = \frac{D_{\text{app}}}{D_{\text{free}}} = \frac{\varrho_{\text{free}}}{\varrho} \tag{8}$$

where D_{free} denotes the diffusion coefficient in the free solution. It should be emphasized that this approach does not include flow caused by capillarity, as in the change from dry to wet concrete, or migration caused by gradients of electrical potential or osmotic pressure, or surface diffusion, as discussed above for the change between distilled water-saturated concrete and seawater-saturated concrete.

This approach has been applied recently [9] to the characterization of cement pastes. For cured cement pastes the diffusibility varies very

strongly with the water/cement ratio (W/C) from around 2×10^{-1} for W/C = 0.7 to about 1×10^{-4} for W/C = 0.2. Diffusibility values for W/C = 0.5–0.55 lie in the range 5×10^{-3} to 2×10^{-2}. In the case of concrete one might expect that diffusibility would be less sensitive to W/C and influenced rather by the packing of the aggregate.

For the concrete used in this study diffusibility values were calculated from the resistivity of seawater saturated specimens. For the non-porous concrete diffusibility was 4×10^{-3} to 1.5×10^{-3} within the range of values exhibited by a cement paste of the same W/C ratio. The diffusibility of the concrete was possibly somewhat lower than that of the cement paste. One might expect this to be the case if the concrete were well packed and free of substantial damage.

For the porous concrete diffusibility was 5×10^{-3} to 2×10^{-2}, a factor of some four times higher than for the non-porous concrete. One would assume that poorer packing of the larger aggregate caused the higher values together with some influence of larger cracks and voids. If resistivities observed between the central rod and outer ring electrodes were taken for the porous concrete specimens, lower values for the diffusibility were obtained. Because of the geometry this measurement sampled essentially only the zone adjacent to the central rod so the implication is that the concrete was much better packed there than the bulk.

5. Conclusion

Impedance measurements executed between electrodes in various types of concrete under different conditions show that the dominating influence is the porosity and, in particular, the cracking of the concrete. Impedance measurements can be used to probe the quality of the concrete and to explore the dynamics of wetting, drying and electrolyte exchange. Interpretation of the phenomena governing these processes may not be straightforward. Corrosion of the electrodes can be detected, but not in a particularly clear cut way – interpretation of a sequence of measurements taken over a period of time is required.

References

[1] F. Mansfield and H. Bertocci (eds), 'Electrochemical Corrosion Testing', ASTM Spec. Publ. 27, American Society for Testing and Materials, Philadelphia (1980).

[2] D. G. John, P. C. Searson and J. L. Dawson, *Br. Corros. J.* **16** (1981) 102.

[3] C. L. Page and K. W. J. Treadaway, *Nature* **297** (1982) 109.

[4] A. P. Crane (ed.), 'Corrosion of reinforcement in concrete construction', Ellis Horwood, Chichester (1983).

[5] J. A. Gonzales, S. Algaba and C. Andrade, *Br. Corros. J.* **15** (1980) 135.

[6] Z. P. Bazant, *Proc. Am. Soc. Civ. Eng., Struct. Div.* **105** (1979) 1137.

[7] Z. P. Bazant, *Proc. Am. Soc. Civ. Eng., Struct. Div.*, **105** (1979) 1155.

[8] J. A. Forrester and R. A. Keen, *J. Appl. Chem.* **10** (1960) 358.

[9] A. Atkinson and A. K. Nickerson, *J. Mater. Sci.* **19** (1984) 3068.